Published in final edited form as:
Calcif Tissue Int. 2009 February ; 84(2): 126–137. doi:10.1007/s00223-008-9201-y.

The PHEX Transgene Corrects Mineralization Defects in 9-Month-Old Hypophosphatemic Mice

Adele Boskey,
Musculoskeletal Integrity Program, Hospital for Special Surgery, affiliated with Weill Medical College of Cornell University, 535 East 70th Street, New York, NY 10021, USA

Aaron Frank,
Musculoskeletal Integrity Program, Hospital for Special Surgery, affiliated with Weill Medical College of Cornell University, 535 East 70th Street, New York, NY 10021, USA

Yukiji Fujimoto,
Musculoskeletal Integrity Program, Hospital for Special Surgery, affiliated with Weill Medical College of Cornell University, 535 East 70th Street, New York, NY 10021, USA

Lyudmila Spevak,
Musculoskeletal Integrity Program, Hospital for Special Surgery, affiliated with Weill Medical College of Cornell University, 535 East 70th Street, New York, NY 10021, USA

Kostas Verdelis,
Musculoskeletal Integrity Program, Hospital for Special Surgery, affiliated with Weill Medical College of Cornell University, 535 East 70th Street, New York, NY 10021, USA

Bruce Ellis,
Department of Pediatrics, Yale University, New Haven, CT, USA

Nancy Troiano,
Department of Orthopaedics and Rehabilitation, Yale University, New Haven, CT, USA

William Philbrick, and
Department of Internal Medicine, Yale University, New Haven, CT, USA

Thomas Carpenter
Department of Pediatrics, Yale University, New Haven, CT, USA

Abstract

Hypophosphatemia is an X-linked dominant disorder resulting from a mutation in the PHEX gene. While osteoblast-specific expression of the PHEX transgene has been reported to decrease the phosphate wasting associated with the disease in male hypophosphatemic (HYP) mice, there are reports that the mineralization defect is only partially corrected in young animals. To test the hypothesis that osteoblast-specific expression of the PHEX gene for a longer time would correct the mineralization defect, this study examined the bones of 9-month-old male and female HYP mice and their wild-type controls with or without expression of the transgene under a collagen type I promoter. Serum phosphate levels, alkaline phosphatase activity, and FGF23 levels were also measured. Mineral analyses based on wide-angle X-ray diffraction, Fourier transform-infrared (FT-IR) spectroscopy, and FT-IR imaging confirmed the decreased mineral content and increased mineral crystal size in male HYP humerii compared to wild-type males and females with or without the transgene and in female HYP mice with or without the transgene. There was a significant increase

Correspondence to: Adele Boskey, Boskeya@hss.edu.

in mineral content and a decrease in crystallinity in the HYP males' bones with the transgene, compared to those without. Of interest, expression of the transgene in wild-type animals significantly increased the mineral content in both males and females without having a detectable effect on crystallinity or carbonate content. In contrast to the bones, based on micro-computed tomography and FT-IR imaging, at 9 months there were no significant differences between the HYP and the WT teeth, precluding analysis of the effect of the transgene.

Keywords

Hypophosphatemic rickets; PHEX; Mineralization; X-ray diffraction; FT-IR

Hypophosphatemia (HYP) is an X-linked dominant disorder resulting from loss of function mutations in PHEX (phosphate regulating gene with endopeptidase activity on the X chromosome) [1]. Humans with these mutations have HYP due to renal phosphate wasting and rickets (i.e., they are short, have bone pain, and have dental abscesses) with abnormally low levels of 1,25-dihydroxyvitamin D [2,3]. Treatment with vitamin D is not effective [4] and the disease has previously been referred to as "vitamin D-resistant hypophosphatemic rickets." The mouse model of HYP occurs naturally and is due to a 3' deletion of PHEX [5–8]. HYP mice have been shown to have impaired growth plate cartilage calcification (rickets) and impaired bone mineralization (osteomalacia), with a decreased mineral content and increased mineral crystal size (crystallinity) in their long bones [9]. The teeth of both male and female HYP mice are also reported to be hypomineralized, with dentin crystals larger than those in control animals [10], analogous to what is seen in humans with HYP [11].

Overexpression of PHEX under the control of the β-actin promoter failed to rescue the HYP, although it did partially correct markers of bone turnover and hypocalcemia in 3-month-old male HYP mice [12]. Histologically, wild-type (WT) mice with the transgene (TG) were not distinguishable from WT mice without the TG, suggesting that these corrections were not an indirect effect of the construct. Expression of the TG in HYP mice partially corrected measures of bone mineral density and histological osteomalacia at 3 months, but mineral composition was not assessed.

Overexpression of PHEX under the control of bone-specific promoters (osteocalcin or type I collagen) also did not correct the phosphate wasting. When PHEX expression was driven by type I collagen in 7- to 8-week-old males, the mineralization defect in both bones and teeth based on histology and radiographs was partially corrected [13]. When driven by the osteocalcin promoter [14], again there was a slight improvement in bone mineralization (based on histology and radiography), but at 12 weeks HYP males with the TG still had defective mineralization of their bones and teeth.

We hypothesized that rescue over a longer period of time under control of the bone-specific promoter (type I collagen) would be able to correct the mineralization defect in HYP animals. Several observations led to this hypothesis. First, it is known that even without the TG there is a correction of the decreased mineralization in female HYP animals (both homozygous and heterozygous) but not male animals [15], thus a comparison of male and female animals treated for longer periods of time would separate these effects. Second, exposure to partially corrected circulating phosphate levels for an extended duration may result in the necessary ambient Ca × P availability to more completely correct the lesion. And third, osteoclastic remodeling's increasing over time [16] would be expected to result in a more mature tissue. In this study we focused the assessments on mineral properties in the bones of these mice as assessed by x-ray diffraction (XRD) and Fourier transform infrared spectroscopy (FT-IR) and spectroscopic

imaging [17]. Additionally, we examined the teeth of representative mice by FT-IR and micro-computed tomography to see whether the HYP mineralization phenotype was affected.

Materials and Methods

Generation of Mice

Transgenic mice were created as illustrated in Fig. 1. In brief, the TG construct consisted of a 2.4-kb rat collagen I promoter element [18] driving a 2250-bp human PHEX coding sequence, followed by 2.2 kb of exons, introns, and polyadenylation/transcription termination sites (p/t) from the human growth hormone gene [19]. The TG was excised as a *XhoI/Not*I fragment and microinjected into SJL × C57BL/6 F_2 oocytes as described [19]. Five founder lines of mice were established and TG expression was evaluated by quantitative RNase protection analysis of calvarial RNA with a probe specific for the hGH sequences on the TG message. Two lines displaying fairly robust levels of TG expression were chosen for subsequent breeding experiments. Transgenic mice with human PHEX (hPHEX) driven by a collagen I promoter were cross-bred with hypophosphatemic mice in a mixed background. Expression of the TG was confirmed by mRNA analyses of calvaria. The genotype of individual mice was determined by PCR. There were a total of 27 female offspring and 23 male offspring. Females consisted of 3 WT without the TG, 4 WT with the TG, 16 HYP without the TG, and 4 HYP with the TG. Males included 8 HYP with no TG, 5 HYP with the TG, 7 WT with no TG, and 2 WT with the TG. Animals were given water and standard food, ad libidum, and were sacrificed at 9 months. The Yale Institutional Animal Care and Usage Review Board approved all animal experimentation.

Morphometrics and Dual-Energy X-Ray Absorptiometry (DXA)-Derived Bone Mineral Measures

Standard morphometric measurements (weight, total body length, and tail length) were obtained at 1, 3, and 9 months. Bone mineral density and bone mineral content of the total femur were performed by DXA using a Lunar Piximus animal densitometer (Madison, WI) after anesthesia with ketamine. Scans were performed in all mice at 1 month of age and in limited numbers of mice in each group at 3 and 9 months. Data were recorded by animal number to allow comparisons of individual mice but averaged for each group of male or female animals (WT, WT + TG, HYP, HYP + TG).

Serum Chemistry

Serum was collected from mice at 1, 3, and 9 months by sampling the retro-orbital sinus. Urine was withdrawn from the bladder at sacrifice. Serum and urinary phosphorus were measured using a commercially available Liqui-UV kit (Stanbio, Boerne, TX). Total serum alkaline phosphatase activity and urine and serum creatinine were assessed using Sigma kits employing a plate reader (Titertek Multiscan, Huntsville, AL). Phosphorus excretion index [urine P/(serum P × urine creatinine)] and phosphorous clearance were calculated. Serum FGF23 was measured using an ELISA method that detects the intact molecule (Kainos Laboratories, Tokyo).

Histology and Histomorphometry

The left tibia of each mouse was dissected, cleaned, and fixed in 70% ethanol, then further dehydrated through graded ethanols, cleared in toluene, and embedded in methyl methacrylate [20]. Longitudinal sections were stained with either toluidine blue, pH 3.7, or, in some cases, a combined von Kossa stain with a toluidine blue counterstain to better visualize the growth plate. Standard histomorphometric parameters as endorsed by the American Society of Bone and Mineral Research Bone Histomorphometry Committee [21] were analyzed using

Osteomeasure software (Osteometrics, Atlanta, GA). Measurements were performed in an area located ~200 μm distal to the growth plate and included trabecular bone only.

Mineral Characterization

The humerii from all animals and first and second molars from selected animals were used for mineral analyses. The humerii were split into proximal and distal ends. The distal ends of each sample were ground using a mortar and pestle and sieved to provide a uniform particle size. The ground bones were first used for FT-IR spectroscopy. KBr pellets were prepared containing 2 mg bone powder per 200 mg dried spectral-quality KBr (Fisher Chemicals, Springfield, NJ). FT-IR spectra were recorded on a Mattson spectrometer (Mattson Industries, Freemont, CA). Because of the small sample size, after preparation of KBr pellets, the remaining sieved material for three samples per group was combined with similar material from the three distal ends from the same animal, reground, sieved, and subjected to wide-angle XRD using a Brucker AX8 powder diffractometer (Madison, WI) with CuK α radiation.

The remaining proximal ends of the humerii (from male HYP, male HYP + TG, male WT, female HYP, and female HYP + TG) were embedded in polymethyl methacrylate, sectioned transversely at 2–3 μm, and used for FT-IR spectroscopic imaging (FTIRI). The sections were mounted on barium fluoride windows (SpectraTech, Hopewell Junction, NY) and used for FTIRI as described elsewhere [22]. In brief, spectra were acquired with a Perkin Elmer Spectrum Spotlight 300 Imaging System (Perkin Elmer Instruments, Waltham, MA), consisting of a step-scanning FT-IR spectrometer with an MCT (mercury-cadmium-telluride) focal-plane array (FPA) detector placed at an image focal plane of an IR microscope. Images were collected in transmission mode at a spectral resolution of 4 cm^{-1} in the frequency region between 1800 and 720 cm^{-1} with an IR detector pixel size (6.25 × 6.25 μm). Background (BaF_2 window only) and PMMA spectra were collected for each section analyzed, and these spectra were used for correction of the sample spectral data using ISYS software (Spectral Dimensions, Olney, MD). Spectra were baselined and the PMMA contribution was subtracted using ISYS software.

The parameters calculated for each image were mineral-to-matrix ratio (related to mineral content), calculated as the ratio of the integrated area under the phosphate band (920–1180 cm^{-1}) to that of the amide I band (1585– 1720 cm^{-1}), and carbonate-to-phosphate ratio (level of carbonate substitution in the HA crystal), calculated as the ratio of the integrated area of the carbonate peak (855–890 cm^{-1}) to the phosphate area. The crystallinity (XST; related to crystallite size/perfection as determined by XRD) was calculated from the intensity ratio of phosphate subbands at 1030 and 1020 cm^{-1}. The collagen cross-link ratio (XLR) was calculated as the intensity ratio of amide I subbands at 1660 and 1690 cm^{-1}. Means and standard deviations for the three to five images in each bone type were calculated and compared.

Phenotypic Characterization of Teeth

Right hemimandibles were extracted, when available, from 11 animals (1 male WT, 2 male HYP, 1 female WT, 1 female WT + TG, 5 female HYP, and 1 female HYP + TG). The molar-bearing part of the jaws was dissected from the rest and analyzed by micro-computed tomography using a Scanco μCT 35 microCT system (Scanco Medical, Bassersdorf, Switzerland). Scans were performed with a 6-μm voxel size and 0.36-deg rotation step at 55 kVp and 145 μA. After three-dimensional reconstruction of the jaw volumes, individual regions of interest for every first and second molar were defined around the anatomical crowns of the molars, and the distributions of mineral densities within the crown regions were extracted to a spreadsheet as histograms. The distribution of dentin mineral densities from these crowns was well differentiated from the background and the enamel values and was used for separate volume (total number of voxels) and average density calculations within each dental tissue.

Parameters calculated were total crown volume, volume of dentin and enamel within the crown, and average dentin and enamel mineral densities. The same samples were subsequently processed for FTIRI as described above for bone. Crown areas from the first and second molars were analyzed on 2-μm sections with a 6.25-μm spatial resolution and a 4-cm^{-1} wavenumber resolution. Only the pixels corresponding to crown dentin as visible on the mineral:matrix images were processed after spatial masking of the embedding medium background, residual enamel tissue, and root dentin. Average values for dentin mineral crystallinity and carbonate substitution were calculated.

Statistical Evaluation

Mean and standard deviations were calculated for all parameters. Age-dependent differences within groups were determined by repeated-measures ANOVA with posttests based on Bonferroni *t*-test, using Instat2 (Graphpad, Carlsbad, CA). Ordinary ANOVA was used for all parameters measured at 9 months, with Bonferroni $p < 0.05$ accepted as significant.

Results

Morphometrics

Female WT mice were consistently shorter and had lower weights than male WT mice (Table 1). Male HYP mice were lighter and shorter than male WT mice but were not larger than female HYP mice at comparable ages. The presence of the TG had no apparent effect on WT weights and lengths, while these morphometric parameters were corrected, but not normalized, in male HYP mice with the TG (Table 1). By 3 months of age the TG had normalized the overall length of both male and female HYP mice, and this correction persisted until sacrifice at 9 months of age. The bone mineral density at 1 month was lower in female than in male WT, and significantly decreased in male HYP but not female HYP mice (Table 1). Expression of the TG in the HYP mice significantly increased the bone mineral density values, but at 1 month these values did not reach those of the male WT. Because of the small sample size at later time points no other significant findings were noted.

Serum Chemistry

Serum phosphate in male HYP animals was significantly lower than in male WT at each age examined (Table 2). Phosphate levels in male HYP with the TG were slightly, but not significantly, higher than in male HYP mice without the TG. In the females the HYP phosphate levels were significantly lower than in the WT at 1 and 3 months but were comparable to those in WT at 9 months. At 9 months, the presence of the TG normalized the phosphate levels in the HYP animals, making them equivalent to values in the WT. Renal clearance of phosphate (at 9 months) appeared greater in all HYP animals compared to the WT, but because of the small sample size this was not significant. Similarly renal clearance of phosphate was not affected by the presence of the TG.

Male HYP mice had significantly higher total serum alkaline phosphatase activity than the male WT at 1 and 3 months (Table 2). Differences at 9 months were not significant, suggesting normalization. In general, in female HYP animals, alkaline phosphatase activity was increased relative to that in the WT, but because of the small sample size due to hemolysis in the 3-month samples, this was not significant.

Serum FGF23 levels at 9 months of age are shown in Fig. 2. As expected [23], HYP mice had significantly ($p < 0.01$) higher circulating FGF23 levels than WT mice, regardless of TG or sex status. FGF23 levels were higher in male Hyp mice than in female Hyp mice ($p < 0.05$). This sex difference was evident when comparing mice that did not express the TG as well as those that were " rescued" with the TG. Furthermore, targeted overexpression of hPHEX in

HYP mice decreased circulating FGF23 (from 818 ± 196 [mean ± SD] to 668 ± 291 pg/ml in males and from 616 ± 220 to 288 ± 44 pg/ml in females). Despite this reduction in circulating FGF23, levels remained markedly elevated in "rescued" HYP mice, and there was no overlap of the range of circulating FGF23 levels in rescued HYP mice compared with WT mice. FGF23 levels in male WT mice expressing the TG (40 ± 13 pg/ml) were somewhat lower than those in male WT ± TG mice (90 ± 34 pg/ml). Although there was no overlap in range of these values, with the substantial variance and small sample size, the significance of this finding is not clear at present. The effect of expression of the TG in female WT mice was not evident.

Histology and Histomorphometry

HYP animals ' bones showed evidence of extensive osteomalacia (Fig. 3) not noted in the animals with the TG. Based on quantitative histomorphometry, expression of the TG only partially corrected the morphometric osteomalacia in the bones of animals with the TG at 9 months (Table 3). In the male WT, the TG had no significant effect on any of the histomorphometric parameters. In the male HYP expression of the TG normalized all the histomorphometric abnormalities except for percentage osteoid (OV/BV), which was considerably improved (reduced 22%) in the presence of the TG. In females, the osteomalacia was less apparent in HYP animals, although osteoid area/tissue area, bone volume fraction, osteoid thickness, and percentage osteoid were significantly increased. Expression of the TG in female HYP reduced the histomorphometric evidence of osteomalacia, but this was statistically significant only for osteoid area/tissue area because of the small number of samples.

In the teeth of 9-month-old animals (Fig. 4) there were no significant differences between the HYP and the WT, with the exception of a slightly (~ 5%) lower mineral density in molars of male HYP compared to the male WT. This was true both for dentin and enamel volumes and for FTIRI results. Figure 4a and b illustrate the methodology for micro-CT evaluation. Table 4 summarizes the FTIRI and micro-CT results for male and female WT and male and female HYP mice. Since there were no phenotypic differences between WT and HYP molars at this age, it was not possible to look for rescue in animals that received the TG.

Mineral Properties

The crystal size/perfection in the HYP males' humerii as determined by XRD line broadening analysis was significantly greater than that in the WT (without the TG). However, there were no significant differences among the other crystal size and perfection measurements for males (Fig. 5). In females, expression of the TG in HYP animals decreased the average crystal size/perfection.

These changes in crystal size/perfection were confirmed by FT-IR analyses of the powdered bones (Fig. 6) and by FTIRI (Fig. 7). FT-IR analysis of crystallinity showed significant differences in HYP males with versus without the TG, with animals with the TG having smaller/less perfect crystals. There was a trend for the TG to reduce the crystal size in female HYP bones and in WT bones of both genders (Fig. 7a), however, the only significant finding was the correction of size in HYP bones by expression of the TG. The mineral content of the humerii, as demonstrated by FT-IR, was decreased in both male and female HYP mice and increased to levels comparable to that in the WT by expression of hPHEX with the TG (Fig. 7b). There were no significant differences between carbonate/phosphate levels in any group, although levels in females tended to be higher than those in males of a similar phenotype (data not shown).

The FT-IR images of each of the parameters showed that the mineral content was decreased in the cancellous and cortical bone of the HYP animals and increased by expression of the TG (Fig. 7a). Bar graphs summarizing the mean values for all data in the images provide a

quantitative basis for this statement (Fig. 7b). Similarly, the TG decreased the average crystallinity (Fig. 7c). Carbonate/phosphate, carbonate/amide I, and collagen maturity were not significantly different (data not shown).

Discussion

These studies have demonstrated that both male and female HYP mice at 9 months of age have a mineral phenotype that is corrected by osteoblast-specific expression of the hPHEX gene. The morphometric phenotype and the serum chemistry, however, are not fully corrected. Previous studies [9] using XRD and chemical analyses showed increased crystal size and decreased ash weight in the bones of young male HYP mice. With the exception of studies by Meyer and collaborators [15,24,25], which reported various extents of sexual dimorphism in shape, ash weight, and mechanical properties of male and female HYP mice, and Abe's study of the teeth, which found that male and female HYP teeth were similar [10], most earlier studies were focused on males because of the likelihood of having more consistently severe disease due to the hemizygous presence of only one X chromosome and, therefore, no normal allele for the PHEX gene. This is in contrast to heterozygous females, which have one normal and one abnormal PHEX allele.

These studies using a combination of morphometric and physical chemical methods to evaluate calcified tissues show that marked correction of the mineral defects in HYP bones is achieved over a 9-month period, with quantitative differences in mineral properties significantly diminished by the continued expression of the TG. More interestingly, the TG has detectable effects in the bones of WT animals that provide some insight into the actions of PHEX. Expression of the TG did not significantly correct the HYP in HYP mice, although it did slightly correct alkaline phosphatase levels, consistent with targeting the TG toward osteoblasts and odontoblasts.

Circulating FGF23 is thought to mediate renal phosphate wasting, and perhaps plays a role in the development of skeletal manifestations, independent of resultant ambient HYP [23]. Interestingly, FGF23 is also overexpressed in undifferentiated and early ameloblasts of HYP animals [26]. A controversy in the hypophosphatemic rickets literature regards the "dominant" nature of the disorder: there is a clinical impression that the spectrum of disease severity in males is greater than that in females in XLH and HYP mice. Thus it is of interest that circulating FGF23 levels in male HYP mice are higher than those in females. Moreover, "rescued" male HYP mice have higher concentrations of circulating FGF23 than rescued female HYP mice. FGF23 levels in rescued male HYP mice approximate those in female HYP + TG mice. It is also possible that overexpression of hPHEX in male WT mice may actually further decrease FGF23 levels, although this cannot be concluded from our data.

It is also of interest that FGF23 levels remained quite elevated in rescued HYP mice, yet the skeletal manifestations of the disease were markedly corrected. In addition, there was not a significant correction of serum P levels. Together, these findings provide strong evidence that loss of function of PHEX plays a major and direct role in the genesis of skeletal abnormalities in XLH/HYP, that these abnormalities are not entirely mediated by serum phosphate concentrations, and, furthermore, that they appear to be independent of FGF23 effects.

Studies by Erben et al. [12] of 3-month-old offspring of crosses between male mice expressing human PHEX under the control of a human β-actin promoter (PHEX-tg) and female heterozygous HYP mice (PHEX-tg) reported normal bone and mineral ion homeostasis. HYP mice showed the known phenotype, with reduced body weight, HYP, hyperphosphaturia, and rickets. HYP/PHEX-tg mice had an almost-normal body weight relative to WT controls, a dramatic improvement in femoral BMD, a nearly normal growth plate width, and, despite

remaining disturbances in bone mineralization, almost-normal bone architecture and pronounced improvements of osteoidosis and of the undermineralized halo formed by the osteomalacic rim of the osteocytic lacunae and typically observed in HYP mice. However, HYP and HYP/PHEX-tg mice had comparable reductions in tubular reabsorption of phosphate and were hypophosphatemic relative to WT controls. Similarly, expressing PHEX under the control of the collagen I promoter did not correct all the bone and tooth mineralization defects at 3 months [13]. This was explained in part by the possibility that human PHEX does not work efficiently in mice and in part by the possibility that others factor are affected by the loss of PHEX at other sites.

In the two studies of younger HYP animals with osteoblast- and odontoblast-specific expression of PHEX, the “partial normalization” of the mineral was based on qualitative radiographic and histologic evidence. In the present study we provide quantitative data on the mineralized tissues showing a more complete rescue at 9 months. The bone mineral content is fully normalized (i.e., there is no significant difference between HYP + TG and WT, although WT + TG has an even higher mineral content), and the crystal size returned to normal values in HYP + TG animals. This occurs in the absence of a correction of serum phosphate, and thus the correction is not based on a physicochemical correction. In the teeth, HYP and WT animals do not differ at 9 months, thus no effect of the TG could be established.

Given the limited changes in circulating phosphate levels, this observed complete correction of mineral content and ratio to matrix content in the skeleton may be a direct consequence of restoring the local bone action of PHEX in rescued HYP mice bones. One potential mechanism may involve the known interaction of PHEX with matrix extracellular phosphoglycoprotein (MEPE) [27], perhaps preventing MEPE from being degraded. MEPE has been shown to act as an inhibitor of mineralization once fragmented [27]. The N-terminal peptide of MEPE, the ASARM peptide, is an inhibitor of mineralization in culture and in cell-free solution [28–30]. Phosphorylated ASARM can be degraded by PHEX [31], removing the inhibition. It has been suggested that the presence of “minihibins,” peptides released from MEPE and other proteins, is responsible for the impaired mineralization in HYP [28]. Unpublished studies from the authors’ laboratory show that the intact protein promotes mineralization in the presence and absence of hydroxyapatite crystals. To convert MEPE into the inhibiting ASARM peptide, a cleavage is required, suggesting that other proteases are involved in the initial cleavage of MEPE. The impaired mineralization in HYP is likely related to the inability to remove the inhibitory effect of the ASARM peptide. It is also possible that PHEX interacts with other proteins that regulate the mineralization process in a similar fashion [30,32].

The dentin in teeth of animals younger than the 9- month-old HYP mice studied here was described [10,11,13] as being thinner and distinctly hypomineralized with respect to that in WT animals, and to have larger crystal sizes than in the WT. From the micro-CT analysis, which is a powerful tool for quantitation of such morphometric and densitometric measurements in teeth, we were not able to detect any phenotypic WT vs. HYP in 9-month-old molars. Dentin mineral differences were also not present between WT and HYP animals, as concluded by the FTIRI analysis. Since we did not examine the teeth in any other age group, we do not know if the phenotype described previously [10,11,13] was present earlier in our animals and corrected later [33] due to continued dentin and mineral formation in HYP animals.

The differences between male and female HYP animals, and the response to rescue of both the HYP and their WT counterparts, merit comment. While the mosaicism of the X chromosome is likely to contribute to the milder appearance of bone and tooth defects in the females, the influence of estrogen may also be important. Gonadectomy [25] of young animals caused male and females to form their mineralized tissues similarly, whereas in the presence of their ovaries the postpubescent female HYP animals gained mineral, while sham-operated and males

without testes did not. Thus we can speculate that the sexual dimorphism observed in the present study is due, to a great extent, to estrogen effects.

Acknowledgments

This work was supported by NIH Grant DE04141 (A.L.B.), Hospital for Special Surgery Musculoskeletal Repair and Regeneration Core Center Grant NIH P30-AR046121 (A.L.B.), and the Traveler's Summer Fellowship Program (A.F.), NIH Center for Research Translation Award P50-AR054086 (T.O.C.), and the Yale Core Center for Musculoskeletal Disorders (NIH P30-AR46032).

References

1. Baum M, Syal A, Quigley R, Seikaly M. Role of prostaglandins in the pathogenesis of X-linked hypophosphatemia. Pediatr Nephrol 2006;21:1067–1074. [PubMed: 16721588]
2. Holm IA, Huang X, Kunkel LM. Mutational analysis of the PEX gene in patients with X-linked hypophosphatemic rickets. Am J Hum Genet 1997;60:790–797. [PubMed: 9106524]
3. Beck L, Soumounou Y, Martel J, Krishnamurthy G, Gauthier C, Goodyer CG, Tenenhouse HS. Pex/PEX Tissue distribution and evidence for a deletion in the 3' region of the Pex gene in X-linked hypophosphatemic mice. J Clin Invest 1997;99:1200–1209. [PubMed: 9077527]
4. Glorieux FH, Holick MF, Scriver CR, DeLuca HF. X-linked hypophosphataemic rickets: inadequate therapeutic response to 1, 25-dihydroxycholecalciferol. Lancet 1973;2:287–289. [PubMed: 4124774]
5. Eicher EM, Southard JL, Scriver C, Glorieux FH. Hypophosphatemia: mouse model for human familial hypophosphatemic (vitamin D-resistant) rickets. Proc Natl Acad Sci USA 1976;73:4667–4671. [PubMed: 188049]
6. Rowe PS, Oudet CL, Francis F, Sinding C, Pannetier S, Econs MJ, Strom TM, Meitinger T, Garabedian M, David A, Macher MA, Questiaux E, Popowska E, Pronicka E, Read AP, Mokrzycki A, Glorieux FH, Drezner MK, Hanauer A, Lehrach H, Goulding JN, O'Riordan JL. Distribution of mutations in the PEX gene in families with X-linked hypophosphataemic rickets (HYP). Hum Mol Genet 1997;6:539–549. [PubMed: 9097956]
7. Du L, Desbarats M, Viel J, Glorieux FH, Cawthorn C, Ecarot B. cDNA cloning of the murine Pex gene implicated in X-linked hypophosphatemia and evidence for expression in bone. Genomics 1996;36:22–28. [PubMed: 8812412]
8. Guo R, Quarles LD. Cloning and sequencing of human PEX from a bone cDNA library: evidence for its developmental stage-specific regulation in osteoblasts. J Bone Miner Res 1997;12:1009–1017. [PubMed: 9199999]
9. Boskey AL, Gilder H, Neufeld E, Ecarot B, Glorieux FH. Phospholipid changes in the bones of the hypophosphatemic mouse. Bone 1991;12:345–351. [PubMed: 1782102]
10. Abe K, Ooshima T, Masatomi Y, Sobue S, Moriwaki Y. Microscopic and crystallographic examinations of the teeth of the X-linked hypophosphatemic mouse. J Dent Res 1989;68:1519–1524. [PubMed: 2584519]
11. Abe K, Ooshima T, Sobue S, Moriwaki Y. The crystallinity of human deciduous teeth in hypophosphataemic vitamin D-resistant rickets. Arch Oral Biol 1989;34:365–372. [PubMed: 2556984]
12. Erben RG, Mayer D, Weber K, Jonsson K, Juppner H, Lanske B. Overexpression of human PHEX under the human beta-actin promoter does not fully rescue the Hyp mouse phenotype. J Bone Miner Res 2005;20:1149–1160. [PubMed: 15940367]
13. Bai X, Miao D, Panda D, Grady S, McKee MD, Goltzman D, Karaplis AC. Partial rescue of the Hyp phenotype by osteoblast-targeted PHEX (phosphate-regulating gene with homologies to endopeptidases on the X chromosome) expression. Mol Endocrinol 2002;16:2913–2925. [PubMed: 12456809]
14. Liu S, Guo R, Tu Q, Quarles LD. Overexpression of Phex in osteoblasts fails to rescue the Hyp mouse phenotype. J Biol Chem 2002;277:3686–3697. [PubMed: 11713245]
15. Brault BA, Meyer MH, Meyer RA Jr, Iorio RJ. Mineral uptake by the femora of older female X-linked hypophosphatemic (HYP) mice but not older male HYP mice. Clin Orthop Relat Res 1987;222:289–299. [PubMed: 3040311]

16. Cao JJ, Wronski TJ, Iwaniec U, Phleger L, Kurimoto P, Boudignon B, Halloran BP. Aging increases stromal/osteoblastic cell-induced osteoclastogenesis and alters the osteoclast precursor pool in the mouse. J Bone Miner Res 2005;20:1659–1668. [PubMed: 16059637]
17. Boskey AL, Young MF, Kilts T, Verdelis K. Variation in mineral properties in normal and mutant bones and teeth. Cells Tissues Organs 2005;181:144–153. [PubMed: 16612080]
18. Pavlin D, Lichtler AC, Bedalov A, Kream BE, Harrison JR, Thomas HF, Gronowicz GA, Clark SH, Woody CO, Rowe DW. Differential utilization of regulatory domains within the alpha 1(I) collagen promoter in osseous and fibroblastic cells. J Cell Biol 1992;116:227–236. [PubMed: 1730746]
19. Wysolmerski JJ, Broadus AE, Zhou J, Fuchs E, Milstone LM, Philbrick WM. Overexpression of parathyroid hormone-related protein in the skin of transgenic mice interferes with hair follicle development. Proc Natl Acad Sci USA 1994;91:1133–1137. [PubMed: 7508121]
20. Kacena MA, Troiano NW, Wilson KM, Coady CE, Horowitz MC. Evaluation of two different methylmethacrylate processing, infiltration, and embedding techniques on the histological, histochemical, and immunohistochemical analysis of murine bone specimens. J Histotechnol 2004;27:119–130.
21. Parfitt AM, Drezner MK, Glorieux FH, Kanis JA, Malluche H, Meunier PJ, Ott SM, Recker RR. Bone histomorphometry: standardization of nomenclature, symbols, and units. J Bone Miner Res 1987;2:595–610. [PubMed: 3455637]
22. Boskey AL, Mendelsohn R. Infrared spectroscopic characterization of mineralized tissues. Vib Spectrosc 2005;38:107–114. [PubMed: 16691288]
23. Yu X, White KE. FGF23 and disorders of phosphate homeostasis. Cytokine Growth Factor Rev 2005;16:221–232. [PubMed: 15863037]
24. Camacho NP, Rimnac CM, Meyer RA Jr, Doty S, Boskey AL. Effect of abnormal mineralization on the mechanical behavior of X-linked hypophosphatemic mice femora. Bone 1995;17:271–278. [PubMed: 8541141]
25. Soener S, RA, Meyer MH, Meyer RA Jr. Ovariectomy abolishes the normalization of femoral mineral content in 40-week-old female X-linked hypophosphatemic mice. Miner Electrolyte Metab 1988;14:321–331. [PubMed: 3231184]
26. Onishi T, Umemura S, Shintani S, Ooshima T. Phex mutation causes overexpression of FGF23 in teeth. Arch Oral Biol 2008;53:99–104. [PubMed: 17942069]
27. Rowe PS, Garrett IR, Schwarz PM, Carnes DL, Lafer EM, Mundy GR, Gutierrez GE. Surface plasmon resonance (SPR) confirms that MEPE binds to PHEX via the MEPE-ASARM motif: a model for impaired mineralization in X-linked rickets (HYP). Bone 2005;36:33–46. [PubMed: 15664000]
28. Rowe PS, Kumagai Y, Gutierrez G, Garrett IR, Blacher R, Rosen D, Cundy J, Navvab S, Chen D, Drezner MK, Quarles LD, Mundy GR. MEPE has the properties of an osteoblastic phosphatonin and minhibin. Bone 2004;34:303–319. [PubMed: 14962809]
29. Martin A, David V, Laurence JS, Schwarz PM, Lafer EM, Hedge AM, Rowe PS. Degradation of MEPE, DMP1 and release of SIBLING ASARM-peptides (minhibins): ASARM-peptide(s) are directly responsible for defective mineralization in HYP. Endocrinology 2008;149:1757–1772. [PubMed: 18162525]
30. Qin C, D'Souza R, Feng JQ. Dentin matrix protein 1 (DMP1): new and important roles for biomineralization and phosphate homeostasis. J Dent Res 2007;86:1134–1141. [PubMed: 18037646]
31. Addison WN, Nakano Y, Loisel T, Crine P, McKee MD. MEPE-ASARM peptides control extracellular matrix mineralization by binding to hydroxyapatite: an inhibition regulated by PHEX cleavage of ASARM. J Bone Miner Res 2008;23:1638–1649. [PubMed: 18597632]
32. Boskey AL. Mineralization of bones and teeth. Elements 2007;3:387–393.
33. Liu S, Tang W, Zhou J, Vierthaler L, Quarles LD. Distinct roles for intrinsic osteocyte abnormalities and systemic factors in regulation of FGF23 and bone mineralization in Hyp mice. Am J Physiol Endocrinol Metab 2007;293:E1636–E1644. [PubMed: 17848631]

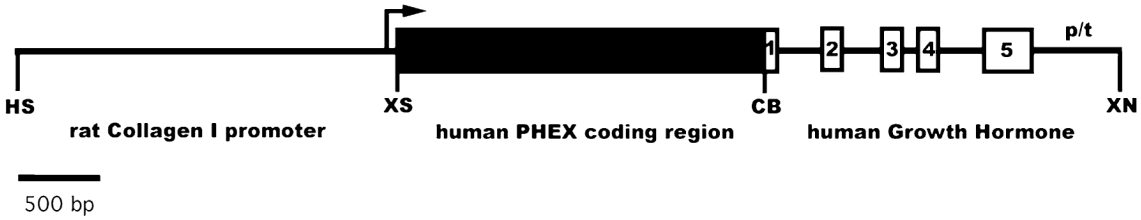

Fig. 1.

Structure of the human PHEX transgene. Diagram of the transgene construct, which consists of a 2.4-kb rat collagen I promoter element driving a 2250-bp human PHEX coding sequence, followed by 2.2 kb of exons, introns, and polyadenylation/transcription termination sites (p/t) from the human growth hormone (hGH) gene. The growth hormone exons (boxed and numbered) are not translated. Restriction sites: B, *Bam*HI; C, *Cla*I; H, *Xho*I; N, *Not*I; S, *Sal*I; X, *Xba*I. The transgene was excised as a *XhoI/Not*I fragment and microinjected into SJL × C57BL/6 F_2 oocytes

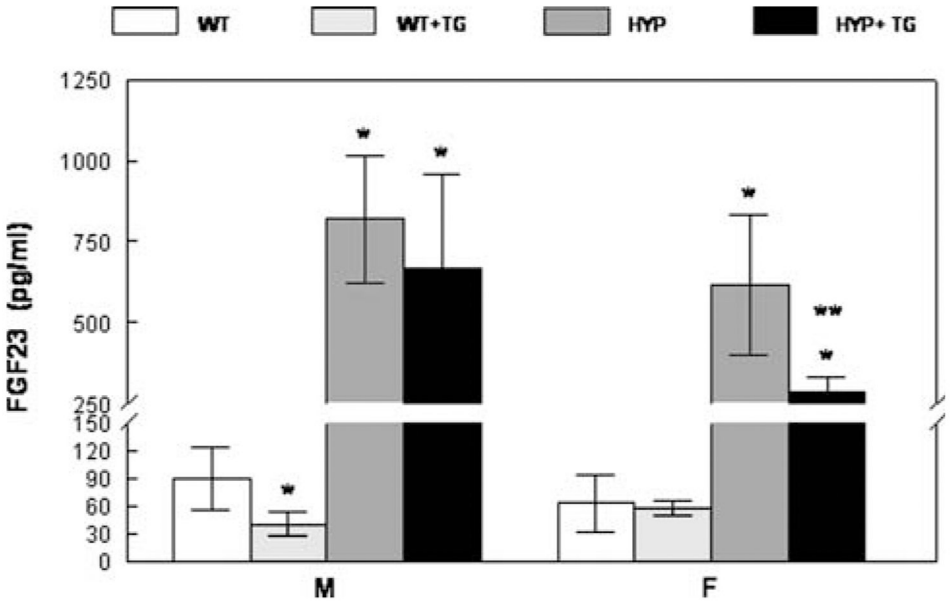

Fig. 2.

Serum FGF23 levels in 9-month-old mice. Mean ± SD. *$p < 0.01$ vs. WT; **$p < 0.03$ vs. HYP of the same gender

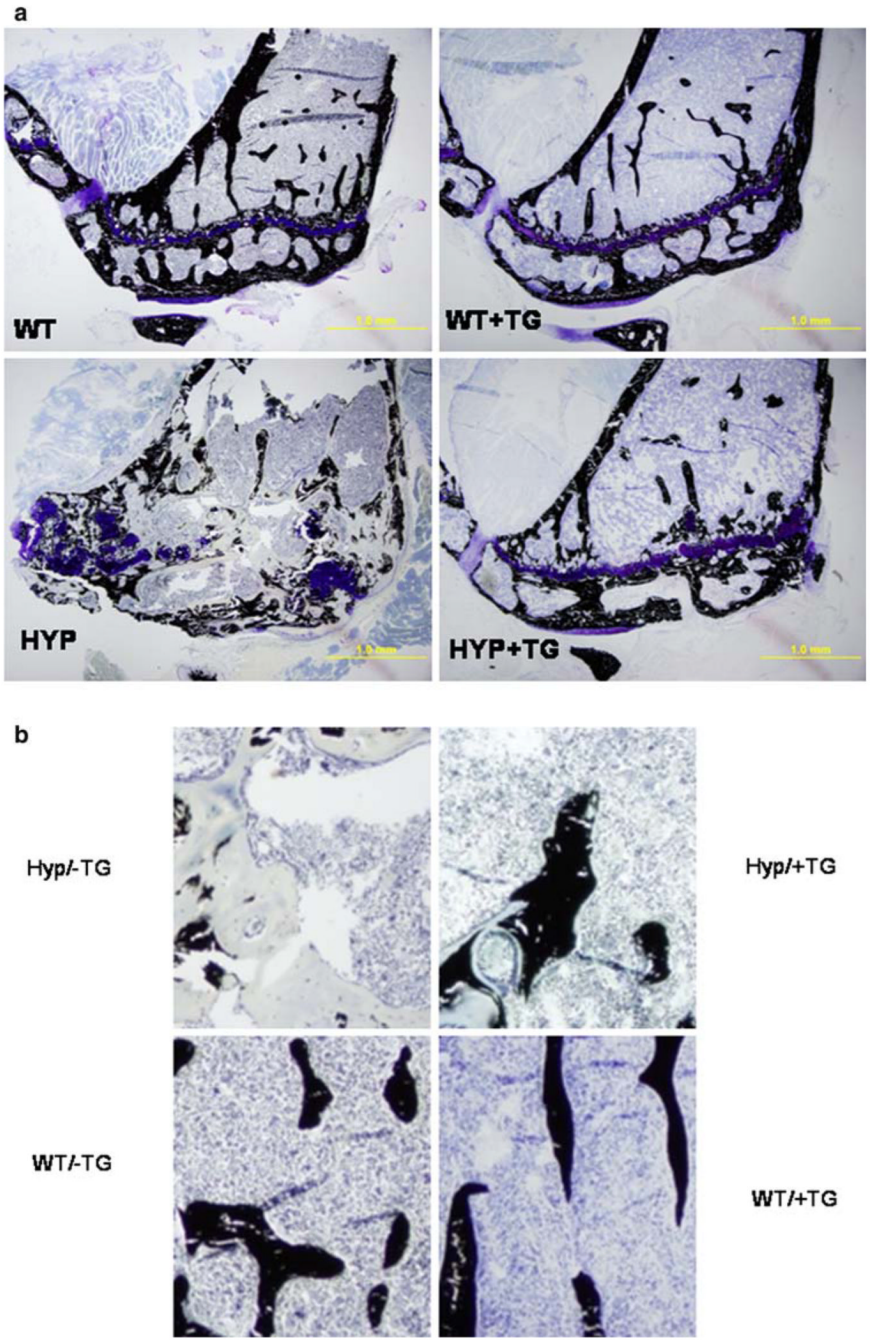

Fig. 3.

Histologic demonstration that expression of the transgene corrects the osteomalacia in the HYP animal but has no apparent effect on the WT. **a** von Kossa-stained sections showing the tibia of 9-month-old male HYP and WT animals with and without expression of the transgene (TG). **b** Higher-power view of the same sections

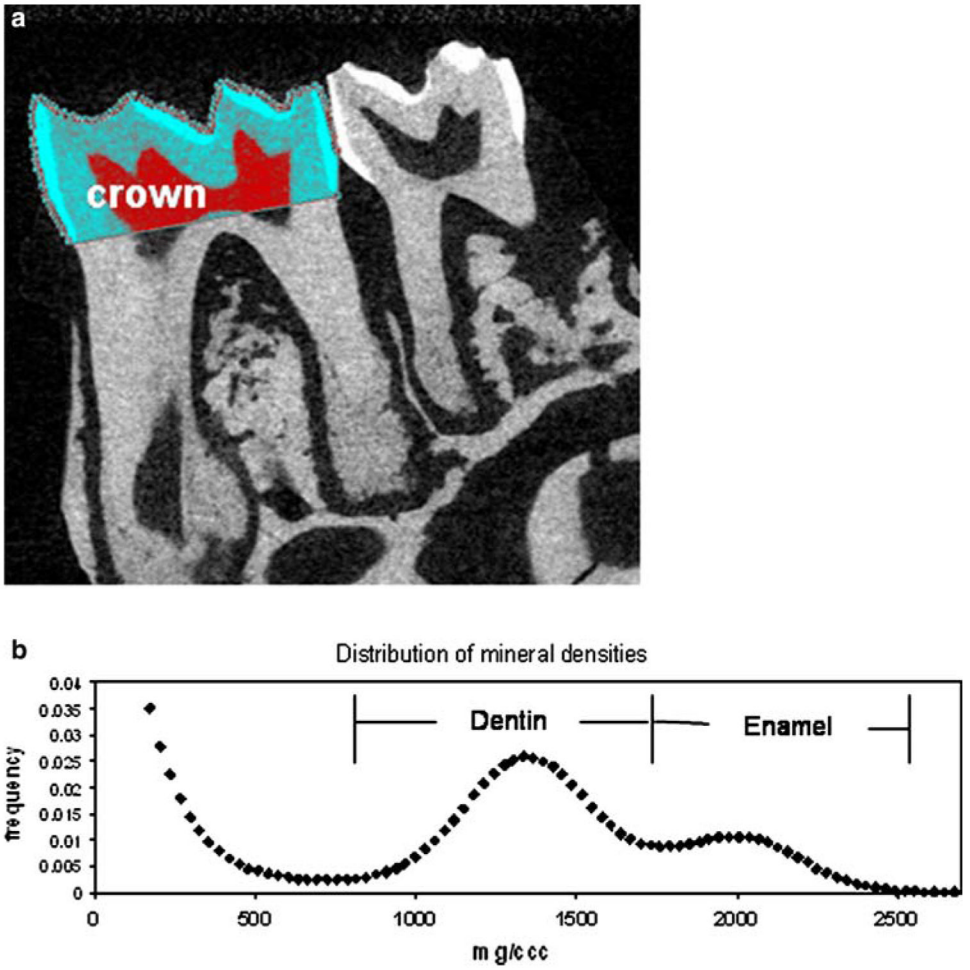

Fig. 4.

Micro-CT evaluation of a mouse molar. **a** Crown region of interest in a first molar defined in a sagittal micro-CT projection of a mouse jaw. **b** Distribution of mineral densities for the crown shown. Note the distinct distributions for dentin and enamel

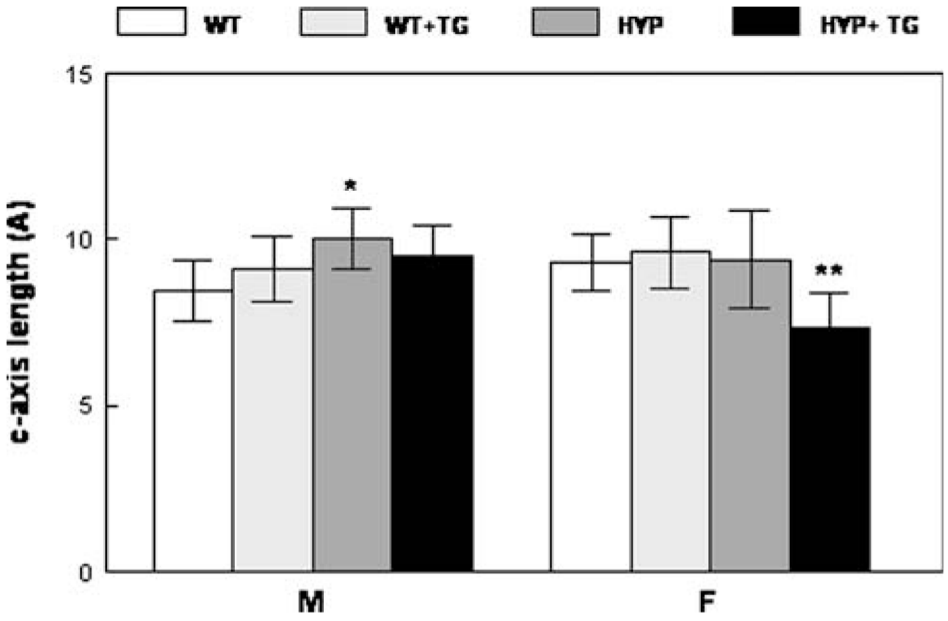

Fig. 5.

X-ray diffraction analyses of 9-month-old humerii demonstrate that expression of the hPHEX transgene normalizes the average crystallite size in the male and female. Mean ± SD. *$p < 0.01$ relative to WT; **$p < 0.01$ relative to same genotype without the transgene

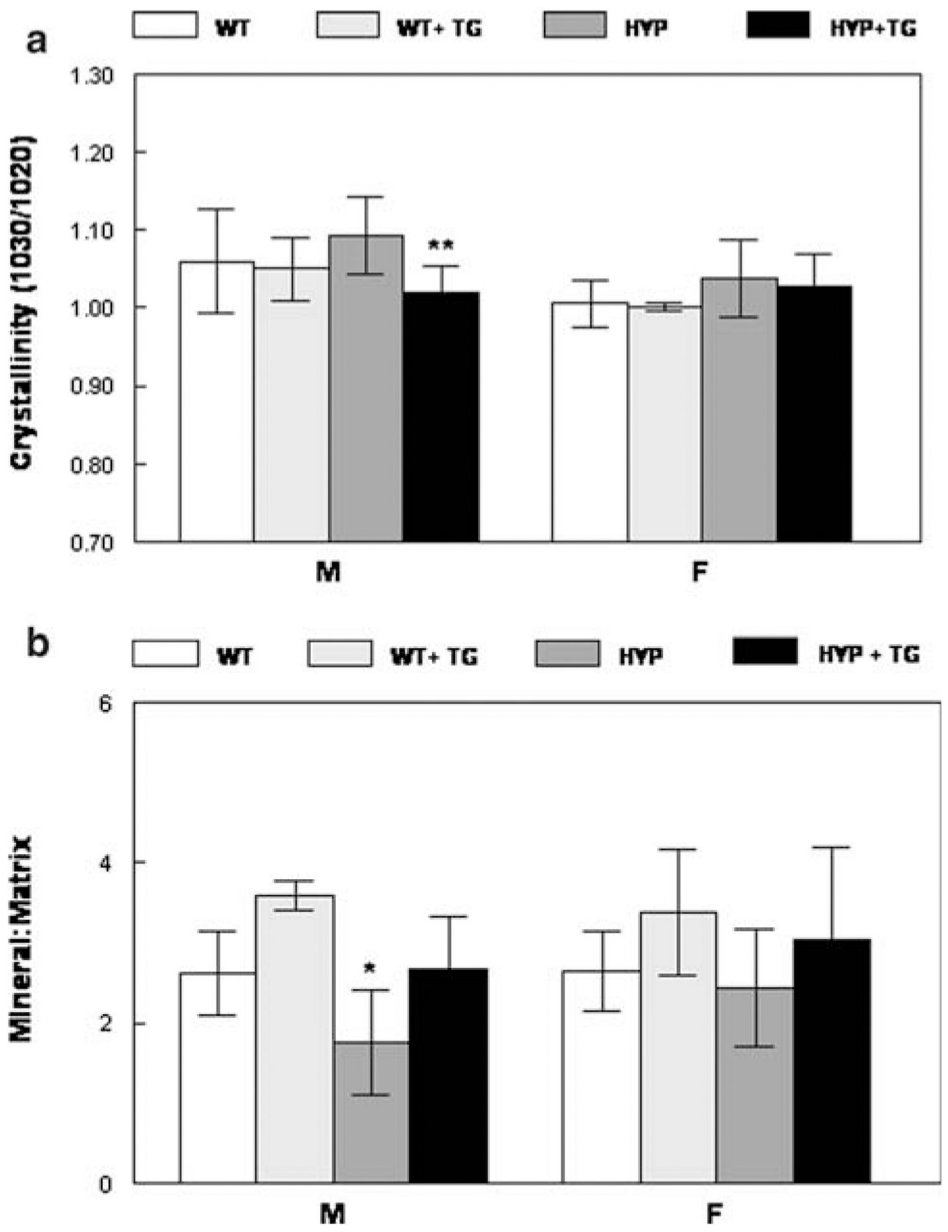

Fig. 6.

FT-IR analyses of ground powders demonstrates that expression of the hPHEX transgene **a** reduces the crystal size and perfection (crystallinity) and **b** increases the mineral content in the HYP humerii. Mean ± SD. *$p < 0.01$ relative to WT; **$p < 0.01$ relative to same genotype without the transgene

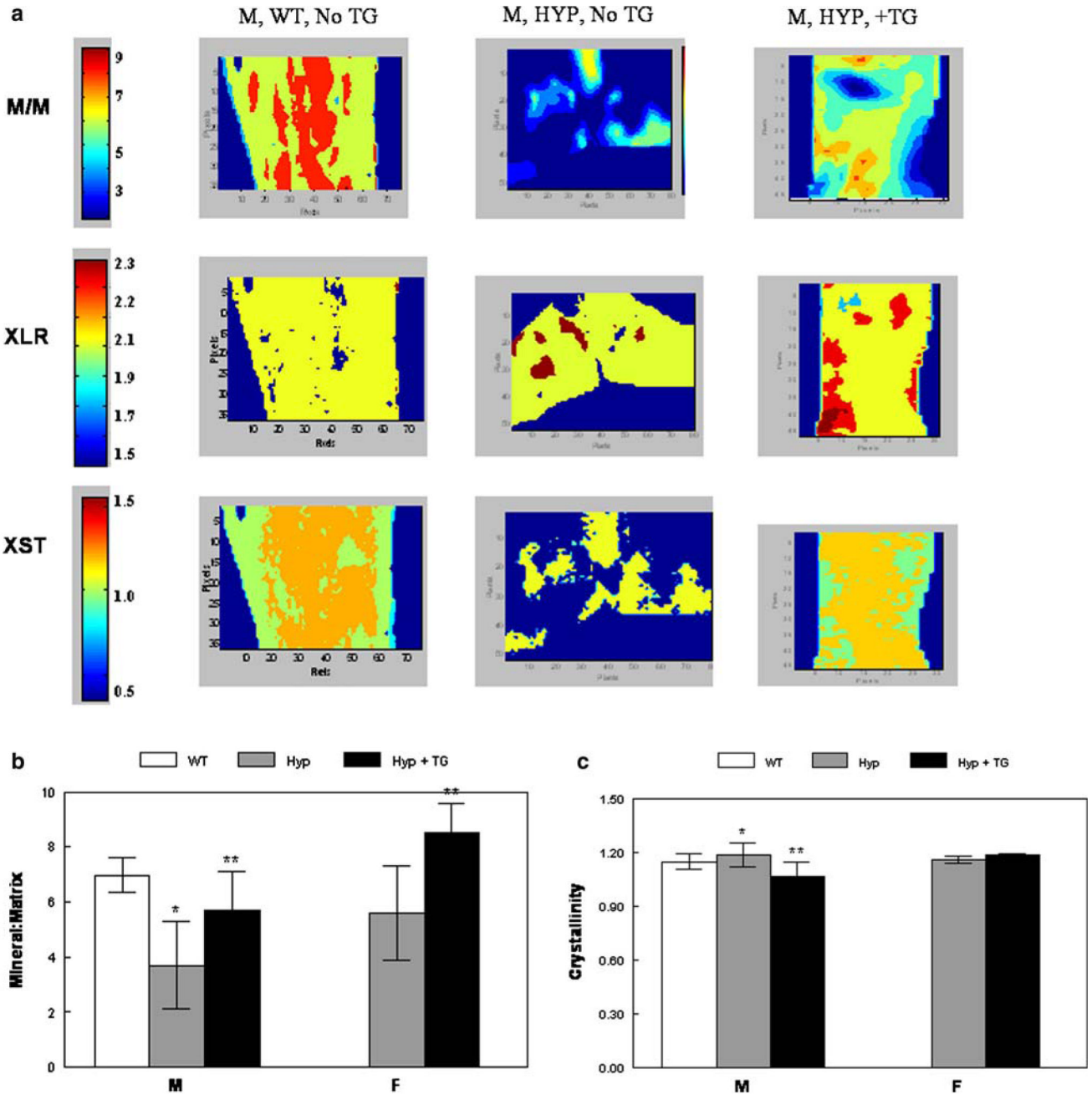

Fig. 7.

Infrared imaging spectroscopy. **a** Typical images showing the distribution of mineral parameters in male HYP, WT, and HYP + TG and female HYP and HYP + TG humerii. Mean and SD for multiple images are summarized for **b** mineral/matrix and **c** crystallinity. *$p < 0.01$ relative to WT; **$p < 0.01$ relative to same genotype without the transgene

Table 1

Morphometric features of HYP/PHEX mice at 1, 3, and 9 months

	WT		HYP		WT + TG		HYP + G	
	Male	**Female**	**Male**	**Female**	**Male**	**Female**	**Male**	**Female**
N	5	9	8	11	4	4	5	4
Body weight (g)								
1 month	23.4 ± 2.5	17.4 ± 1.6	**19.0 ± 1.0**	17.1 ± 1.4	23.5 ± 1.5	17.8 ± 1.0	21.2 ± 1.2	18.5 ± 2.4
3 months	37.0 ± 4.8	22.4 ± 2.6	**25.3 ± 2.4**	22.0 ± 2.8	34.8 ± 2.2	23.4 ± 1.8	**32.2 ± 2.2**	23.3 ± 3.5
9 months	45.0 ± 3.2	27.4 ± 5.9	**28.1 ± 5.2**	26.8 ± 5.1	43.6 ± 3.3	29.8 ± 5.6	38.2 ± 4.8	30.4 ± 11.3
Length of animal (cm)								
1 month	15.7 ± 0.7	13.8 ± 0.8	**13.4 ± 0.4**	13.5 ± 0.8	15.5 ± 0.4	14.7 ± 0.3	**14.4 ± 0.4**	14.5 ± 0.6
3 months	17.5 ± 0.9	15.5 ± 1.1	**14.5 ± 0.6**	14.7 ± 1.1	17.1 ± 0.7	17.2 ± 0.9	16.7 ± 0.9	16.3 ± 0.5
9 months	17.8 ± 0.7	15.3 ± 1.0	**14.0 ± 1.0**	14.7 ± 1.1	17.9 ± 0.7	17.0 ± 1.2	17.0 ± 0.9	16.1 ± 0.7
BMD (g/cm^2)								
1 month	0.040 ± 0.002 (5)[a]	0.031 ± 0.003 (9)	**0.027 ± 0.001 (8)**	0.029 ± 0.002 (11)	0.040 ± 0.002 (4)	0.033 ± 0.005 (4)	**0.032 ± 0.001 (5)**	0.033 ± 0.005 (4)
3 months	ND	0.033 ± 0.002 (2)	0.027 ± 0.001 (2)	0.036 ± 0.008 (5)	0.0299	0.030 ± 0.001 (2)	0.044 ± 0.0004 (2)	0.032 ± 0.007 (3)
9 months	ND	0.046 ± 0.005 (2)	0.043 ± 0.003 (2)	0.050 ± 0.009 (5)	0.0388	0.0401 ± 0.001 (2)	0.056 ± 0.0008 (2)	0.041 ± 0.009 (3)

Note: *HYP* hypophosphotemic, *WT* wild type, *TG* transgene, *ND* not determined. Values are mean ± SD for N animals. Values in boldface indicate $p < 0.01$ vs. WT of same sex

[a] *n* for BMD measurements given in parentheses. For values with no SD, $n = 1$

Table 2

Temporal changes in serum inorganic phosphate (Pi) and alkaline phosphatase (AP): mean ± SD (*n*)

Phenotype	1 month		3 months		9 months		
	Pi (mg/dl)	AP (U/L)	Pi (mg/dl)	AP (U/L)	Pi (mg/dl)	AP (U/L)	PIC
Male							
WT	8.6 ± 1.2 (5)	1180 ± 206	9.3 ± 1.2 (5)	610 ± 140	9.4 ± 1.1 (5)	506 ± 43	0.399 ± 0.20 (4)
WT + TG	8.3 ± 1.0 (4)	1217 ± 260	7.8 ± 0.94 (3)	502.0 ± 46.0	8.2 ± 1.7 (4)	454 ± 40	0.46 ± 0.12 (4)
HYP	5.3 ± 0.7*(8)	2484 ± 504*	5.6 ± 1.3*(6)	1196 ± 275*	5.6 ± 1.7*(8)	993 ± 217	0.65 ± 0.37 (5)
HYP + TG	5.7 ± 0.6*(5)	1911 ± 708	5.4 ± 1.4*(3)	733 ± 190	6.7 ± 1.2 (5)	686 ± 60**	0.78 ± 0.84 (3)
Female							
WT	9.0 ± 0.9 (3)	1915 ± 147	7.8 ± 1.5 (3)	708 ± 125	6.1 ± 0.5 (3)	639 ± 110	0.029 ± 0.010 (3)
WT + TG	8.5 ± 1.1 (5)	1765 ± 494	8.2 ± 0.9 (2)	699 ± 187	7.4 ± 1.4 (5)	647 ± 98	0.248 ± 0.19 (3)
HYP	5.3 ± 0.7*(17)	2357 ± 522	5.4 ± 1.1*(11)	1023 ± 250	4.9 ± 4 (17)	910 ± 235	0.67 ± 0.55 (11)
HYP + TG	6.6 ± 0.4*(3)	2558 ± 336	4.7 (1)	780	6.1 ± 1.5 (3)	724 ± 90	0.64 ± 0.88 (2)

Note:PIC phosphate clearance, *WT* wild type, *TG* transgene, *HYP* hypophosphatemia. Samples in which there was obvious hemolysis are not included in these data.

* Significantly different from WT of the same gender.

** Significantly different from same genotype with the TG

Table 3

Histomorphometry of left tibial sections from 9-month-old mice: mean ± SD

	WT	WT + TG	HYP	HYP + TG
Male				
N	5	4	8	5
OV/TV (%)	0.31 ± 0.18	0.44 ± 0.13	24.66 ± 13.95*	5.48 ± 3.36**
BV/TV (%)	19.6 ± 5.35	19.72 ± 4.37	87.5 ± 19.7*	24.7 ± 18.8**
OsTh (μm)	1.72 ± 0.24	2.1 ± 0.39	16.02 ± 6.05*	7.74 ± 1.06**
TbN (per mm^2)	4.1 ± 0.75	4.38 ± 0.67	5.64 ± 0.48	3.87 ± 2.04
OV/BV (%)	1.56 ± 0.80	2.20 ± 0.23	46.44 ± 22.02*	25.49 ± 5.94
Female				
N	4	5	17	3
OV/TV (%)	0.38 ± 0.11	0.29 ± 0.12	11.55 ± 9.4*	2.86 ± 1.33**
BV/TV (%)	12.5 ± 5.02	8.42 ± 2.51	37.1 ± 18.1*	16.9 ± 7.7
OsTh (lm)	2.03 ± 0.32	2.11 ± 0.64	10.02 ± 4.64*	6.01 ± 1.2
TbN (per mm^2)	2.68 ± 0.73	2.14 ± 0.75	4.5 ± 1.52	3.1 ± 0.5
OV/BV (%)	3.17 ± 0.83	3.74 ± 1.88	27.1 ± 12.7*	19.5 ± 10.3

Note: *WT* wild type, *TG* transgene, *HYP* hypophosphatemia, *OV/TV* osteoid area/tissue area, *BV/TV* bone volume/tissue volume, *OsTh* osteoid thickness, *TbN* trabecular number, *OV/BV* percentage osteoid.

* $p < 0.01$ vs. WT;

** $p < 0.01$ vs. same genotype without the TG

Table 4

Micro-computed tomography (CT) and Fourier transform-infrared imaging (FTIRI) analyses of first molars from 9-month-old mice

	WT		HYP	
	Male	**Female**	**Male**	**Female**
Micro-CT				
Crown volume (mm^3)	0.57	0.61 ± 0.05	0.60 ± 0.01	0.63 ± 0.03
Dentin volume (mm^3)	0.34	0.37 ± 0.04	0.32 ± 0.01	0.35 ± 0.02
Enamel volume (mm^3)	0.11	0.13 ± 0.01	0.09 ± 0.01	0.10 ± 0.01
Average dentin mineral density (mg/cm^3)	1355	1353 ± 8	1333 ± 2	1330 ± 13
Average enamel mineral density (mg/cm^3)	2029	2036 ± 1	2007 ± 17	2024 ± 20
Dentin FTIRI (relative scale)				
Mineral crystallinity	1.11	1.13 ± 0.09	1.14 ± 0.02	1.08 ± 0.03
Carbonate-to-phosphate ($\times 10^{-4}$)	70	72 ± 11	72 ± 8	74 ± 9

Note: *WT* wild type, *HYP* hypophosphatemia